Particle confinement isotope effect in FT-2 tokamak

A.D. Gurchenko[1], E.Z. Gusakov[1], P. Niskala[2], A.B. Altukhov[1], L.A. Esipov[1], M.Yu. Kantor[1], T.P. Kiviniemi[2], T. Korpilo[2], D.V. Kouprienko[1], S.I. Lashkul[1], S. Leerink[2], R. Rochford[2], L. Chôné[2], G.A. Troshin[1], V.A. Ivanov[1]

[1] *Ioffe Institute, St. Petersburg, Russia*

[2] *Aalto University, Espoo, Finland*

A new wave of interest has been raised in last few years to the isotope effect in a tokamak confinement which remains a long-standing puzzle for the period of 40 years, within which the energy anomalous transport decrease was observed in numerous experiments with growth of the hydrogen isotope number in contradiction to the theory expectations. The novel approach to explanation of this effect, which is favourable for fusion applications, is based on accounting for the multi-scale turbulence nonlinear interactions, in particular, for the coupling between small-scale turbulence and zonal flows.

In this paper the isotope effect in particle confinement is investigated experimentally in FT-2 tokamak ($R = 55$ cm, $a = 7.9$ cm) with a circular limiter and computationally by the global gyrokinetic (GK) code ELMFIRE [1, 2]. Experiments were performed in two pairs of similar hydrogen (H) and deuterium (D) ohmic discharges with high and low central density shown in fig. 1(a, b). GK simulations were performed at time moments pointed by black arrows, indicated as NH-ND and GH-GD cases, respectively. The density profiles for these cases are shown in fig. 1(c).

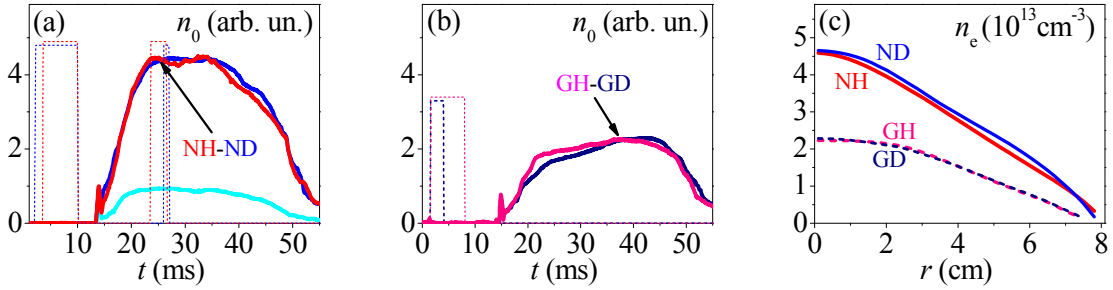

Fig. 1. Waveforms of the central density: (a) high (periods of gas pulse fueling are shown by dashed lines; cyan - profile with minor stationary fueling) and (b) low. (c) Density profiles in "N"- and "G"-cases.

General parameters of these selected cases are presented in the table below.

Case label	Fuel isotope	Plasma Current I_p, kA	Toroidal magnetic field B_t, T	Loop voltage U_L, V	Z_{eff}	$\int PdV$, kW			τ_E, ms
						OH	radiation	e-i collisions	
NH	H	30.5	2.27	3.6	3.8	112	31	9	1.1
ND	D	31.1	2.24	3.8	4.1	119	39	5	1.1
GH	H	32.9	2.17	2.9	2.2	97	7	4	0.7
GD	D	33.5	2.14	3.0	2.2	102	7	3	0.7

Profiles of electron and ion temperatures and radiation power interpolated from experimental ones by ASTRA code [3] and used for transport modelling are shown in

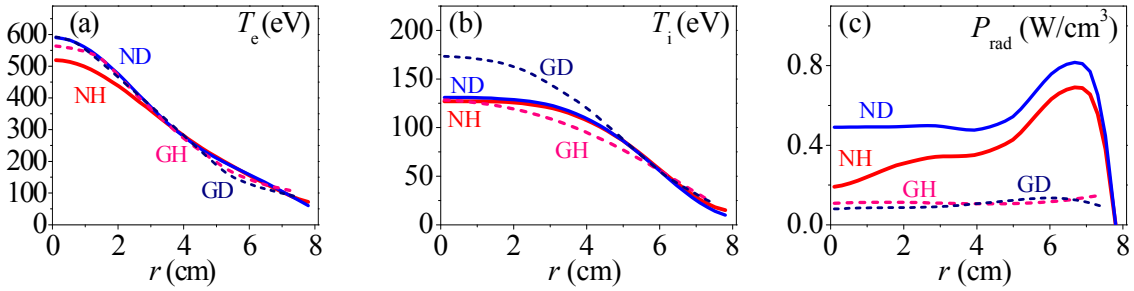

Fig. 2. Profiles of (a) electron, (b) ion temperature and (c) radiation power.

fig. 2. The safety factor profile obtained by ASTRA is shown in fig. 3(a). The energy confinement time τ_E was estimated from the power balance as $\tau_E = W/(P_{OH} - dW/dt)$, where W is the energy content of the plasma. The similarity of the heating power and the energy content for H and D plasmas results in the absence of the favourable isotope effect in the electron energy confinement.

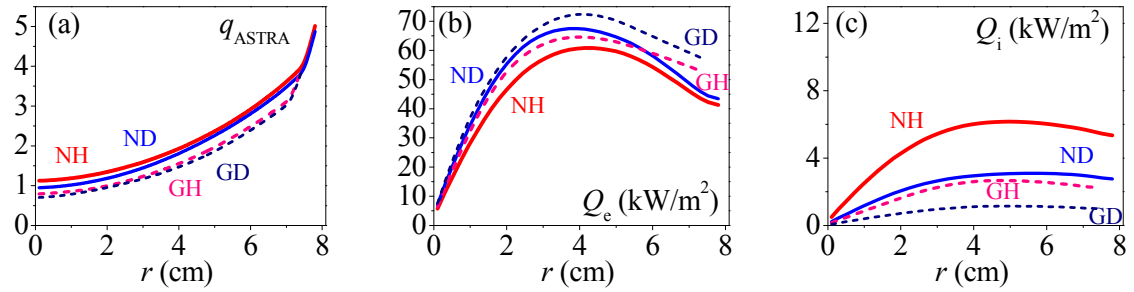

Fig. 3. Profiles of (a) the safety factor, (b) electron and (c) ion energy fluxes estimated by ASTRA.

Electron and ion energy fluxes estimated by ASTRA modelling are shown in fig. 3(b, c). Q_e in D cases exceeds by 10% the corresponding values in H but this difference is less than 15% error in the flux determination. Q_i in NH-ND cases is larger by a factor of 2.3-2.7 than at low density. In both cases fluxes are larger for H compared to D by 50-60%, but it should have only a small effect on the energy confinement, because Q_i values are an order of magnitude smaller than Q_e. Energy fluxes were also investigated in GK computations performed by ELMFIRE particle-in-cell code simulating the full distribution of two GK ion species and drift-kinetic electrons in a global toroidal geometry with circular and concentric flux surfaces and providing the self-consistent evolution of the electrostatic equilibrium and fluctuations [1, 2]. The pronounced isotope effect in electron energy fluxes (fig. 4(a)) was obtained in GK computations in NH-ND cases in contradiction with ASTRA estimations shown in fig. 3(a). The isotope effect in ion channel is also observable in ELMFIRE calculations (fig. 4(6)), but energy fluxes are twice larger than in ASTRA modelling.

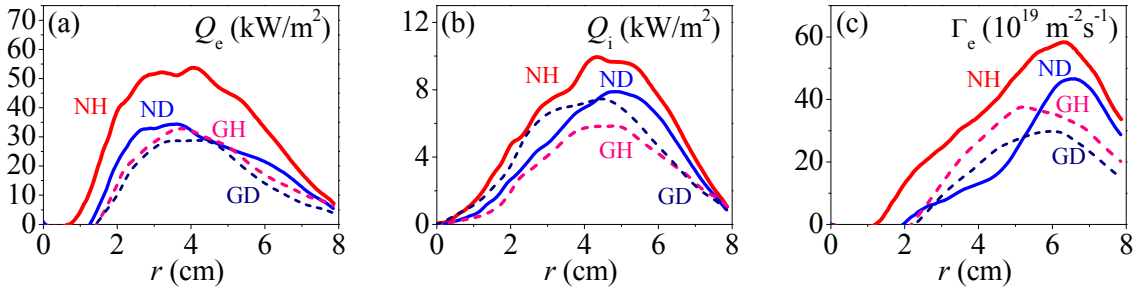

Fig. 4. ELMFIRE simulated profiles of (a) electron and (b) ion energy fluxes and (c) particle flux.

The pronounced isotope effect in particle fluxes was demonstrated in GK simulations both in NH-ND and GH-GD cases (fig. 4(c)). Although the maximum difference between the fluxes in D and H was observed at the middle of the radius in the NH-ND case, it was even smaller than in GH-GD case near the plasma edge at $r > 6.7$ cm. Experimental approach to the particle confinement research utilizes measurements of H_β and D_β radiation lines intensity. This method is based on the fact that the particle balance could be used for estimation of the global particle confinement time $\tau_p = \langle n_e \rangle / \left(\Phi - d\langle n_e \rangle / dt \right)$, where Φ is the particle source. In the steady state the global particle confinement time is determined only by the particle source, which can be characterized by volume integrated H_β and D_β radiation line intensity J, proportional to the ionization rate and neutral particle density determined by recycling and fueling ($\tau_p \sim \Phi^{-1} \sim < J >^{-1}$) [4].

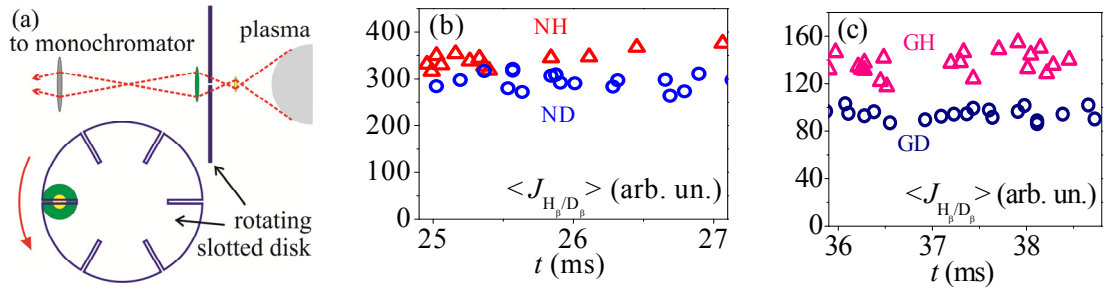

Fig. 5. (a) Scheme for H_β and D_β line intensity measurements, mean J in (b) "N"- and (c) "G"-cases.

The utilized optical scheme is shown in fig. 5(a). The complete vertical scan of the plasma is carried out for 1.3 ms with a periodicity of 3.4 ms by rotating slotted disk. Intensities J averaged over 1.3 ms time intervals are shown in fig. 5(b, c). The clear isotope effect is observed (fig. 5(c)) in GH-GD case: the corresponding relation $\tau_{p\,D} / \tau_{p\,H} \approx 1.5$. As is seen in fig. 5(b) H_β and D_β line intensities in NH-ND case are much closer providing the relation $\tau_{p\,D} / \tau_{p\,H} \leq 1.2$, nevertheless indicating a higher particle source for the lighter isotope and corresponding larger particle flux through the last closed flux surface.

We have previously [5, 6] associated different levels of particle fluxes with the difference in radial turbulent fluxes: $\Gamma_r = \langle \delta n \delta V_r \rangle$. In contrast to the low 19 kA current regime, where

the suppression of the turbulent flux in D compared to H at the same level of density fluctuations δn and radial velocity fluctuations δV_r was due to the phase difference between them (which became closer to 90 degrees in D), in NH case δn was larger than in ND in the inner region (fig. 6(a)) and δV_r was larger both in NH and GH in comparison with ND and GD cases correspondingly (fig. 6(b)) thus explaining the difference in particle fluxes.

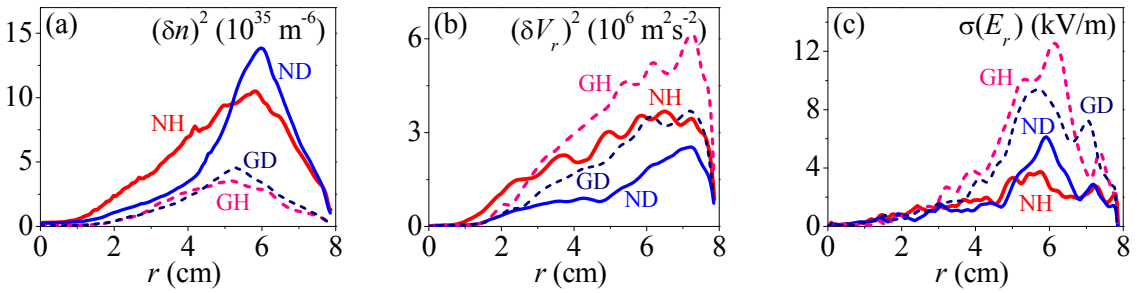

Fig. 6. ELMFIRE profiles of (a) density fluctuations, (b) radial velocity fluctuations, (c) the GAM amplitude.

Zonal flows probably could play a role in the isotope effect [7, 8]. In NH-ND and GH-GD cases the geodesic acoustic mode (GAM) was observed both in the experiment and in the GK computations. The computed amplitude of the radial electric field associated with GAMs is shown in fig. 6(c). It looks more intensive at smaller densities; however GAM amplitudes are comparable in GH and GD cases. In ND case GAM amplitude is in fact larger but only in the narrow region around $r = 6$ cm. It should be mentioned that the effect of the high correlation between the turbulent bursts of transport and GAMs [5, 9] on the particle transport is the subject of the further research.

Co-authors of the paper would like to acknowledge financial support of Russian Science Foundation grant 17-12-01110. The work has been supported by the Academy of Finland grants 278487 and 296853. CSC – IT Center for Science and EUROfusion High Performance Computer (Marconi-Fusion) are acknowledged for allocation of computational resources for this work.

[1] Heikkinen J.A. et al. 2008 J. *Comput. Phys.* **227** 5582

[2] Korpilo T. et al. 2016 *Comput. Phys. Commun.* **203** 128

[3] Pereverzev G.V. and Yushmanov P.N. 2002 IPP 5/98 Preprint Garching

[4] Liu B. et al. 2016 *Nucl. Fusion* **56** 056012

[5] Gurchenko A.D. et al. 2016 *Plasma Phys. Control. Fusion* **58** 044002

[6] Niskala P. et al. 2017 *Plasma Phys. Control. Fusion* **59** 044010

[7] Xu Y. et al. 2013 *Phys. Rev. Lett.* **110** 265005

[8] Hahm T.S. et al. 2013 *Nucl. Fusion* **53** 072002

[9] Gurchenko A.D. et al. 2015 *Europhys. Lett.* **110** 55001